N·H

ELSEVIER

High resolution measurements of neutron energy spectra from Am–Be and Am–B neutron sources

J.W. Marsh[1,*], D.J. Thomas, M. Burke

Division of Radiation Science and Acoustics, National Physical Laboratory, Teddington, Middlesex, TW11 0LW, UK

Abstract

A ^{3}He sandwich spectrometer incorporating two semiconductor detectors and a proportional counter region has been designed and constructed to perform high resolution measurements of neutron energy spectra in the energy range 100 keV to 15 MeV. The efficiency of the spectrometer was determined experimentally, using a ^{252}Cf spontaneous fission source, in the low-scatter facility of the National Physical Laboratory. The Monte Carlo technique was also used to determine the efficiency and these calculated values were used to extrapolate the measured efficiency to higher energies. The neutron energy spectra from two different sized Am–Be neutron sources and an Am–B neutron source were measured. Although these spectra have been measured previously, the present work represents an improvement in the energy resolution and extends the energy range. Average values for dose equivalent quantities for neutrons from these sources are also presented. The spectral data is available from the authors, as a printed table or on a computer diskette, on request.

1. Introduction

The National Physical Laboratory (NPL) has several (α,n) neutron sources that produce neutron fields which are well characterised in terms of total neutron emission rate. The variation of neutron emission relative to the axis of the source is also well known and has been measured in a low-scatter area using a DePangher long counter. However, the application of these sources is limited to some extent by the lack of precise knowledge of their energy spectra. Because there is no absolute spectrum common to all (α,n) sources (even those that have the same target element and α-particle emitter can differ in detail) it is necessary to carry out spectral measurements of these neutron sources to define the neutron field completely. The work described here, and in greater detail in Ref. [1], presents the results of high resolution measurements of neutron energy spectra from three neutron sources. These are: a 370 GBq (10 Ci) ^{241}Am–Be source; a 37 GBq (1 Ci) ^{241}Am–Be source; and a 37 GBq (1 Ci) ^{241}Am–B source.

These types of neutron sources have been subject to

a number of energy spectrum measurements. To a certain extent the energy spectrum from radionuclide neutron sources which utilize the Be(α,n) reaction are reasonably well established above 3 MeV. Peaks are observed near 3.1, 4.8, 6.6, 7.7 and 9.8 MeV [2–7]. However, Lorch [8] detected an additional peak at 4.3 MeV from an Am–Be source. It is interesting to note that other authors [9,10] have shown evidence of a similar peak in the 4 to 4.3 MeV region for Am–Be sources of the same construction. This suggests that the detailed shape of the neutron energy spectrum may depend on the way in which the active component is prepared, e.g. the degree of uniformity of the mixture of americium and beryllium, because this influences the distribution of α-particle energies. Van der Zwan [11] demonstrated theoretically that the size of the clusters of the actinide oxide embedded in the beryllium affects the shape of the energy spectrum.

Kluge and Weise [12] were the first to use a ^{3}He sandwich spectrometer to measure the neutron energy spectrum from an Am–Be source. Previous measurements used mainly nuclear emulsions, organic scintillators or recoil proton telescopes. The measurement of Kluge and Weise provided considerable improvement in terms of energy resolution and energy range.

The neutron energy spectrum for Am–B sources, with either natural boron or ^{11}B, consists essentially of a broad peak with no fine structure. The reported

---

* Corresponding author. Tel. +44 1235 831600, fax +44 01235 833891.

[1] Present address National Radiological Protection Board, Chilton, Didcot, Oxfordshire, OX11 0RQ, U.K.

positions and widths of the peak differ considerably [7,13–16]. The position of the peak varies between 2.5 and 3.4 MeV and the FWHM of the neutron distribution varies between 1.5 and 3 MeV. However, the neutron energy spectrum from an Am–B source measured by Werle [15] shows an additional peak at ~340 keV amounting to about 8% of the total neutron intensity. The disintegration mechanism on which this peak is based has not been resolved.

The high resolution measurements presented in this paper have been carried out with a ^{3}He sandwich spectrometer in a low scatter facility at NPL. This spectrometer has an energy range from 100 keV to 15 MeV. For each of the three neutron sources measured, the average neutron energy and values for various dose equivalent quantities are also presented.

2. The ^{3}He spectrometer and its associated instrumentation

A ^{3}He spectrometer has been constructed to an improved design [1], based on the earlier work of Kluge and Weise [12], and Bluhm [17]. It consists of two silicon surface barrier detectors mounted 8 mm apart. The space between them is filled with ^{3}He gas and is operated as a proportional counter. The sensitive volume is thus formed by the wall of the cathode box and the faces of the semiconductor detectors. For ^{3}He(n,p)^{3}H reactions induced in the sensitive volume of the spectrometer the energy loss of the proton and the triton in the gas, $\Delta E = \Delta E_p + \Delta E_t$, is measured by the proportional counter and their residual energies E_p and E_t by the semiconductors. The neutron energy E_n can then be calculated from

$$E_n = E_p + E_t + \Delta E - Q, \text{ where } Q = 763.8 \text{ keV}.$$

The three signals, E_p, E_t and ΔE are read in coincidence. If the proton enters one semiconductor then for a coincidence event to occur the triton must enter the other semiconductor. The three coincidence signals are recorded for each event so that both on-line and off-line data analysis can be performed.

To discriminate against gamma-ray induced events, and (n,α) reactions in the silicon, a two parameter analysis is carried out. The proportional counter pulse (ΔE) is taken as one parameter and the other is the sum of the three detector pulses (E_S). If an electron or an α-particle deposits a similar amount of energy in the gas to a proton plus triton combination then the total energy, E_S will be very different, thereby allowing the two types of event to be distinguished.

To discriminate against (n,p) reactions in the silicon, background measurements are performed with the

spectrometer filled with ^{4}He and these are then subtracted from the spectrum measured with ^{3}He.

2.1. Design considerations

A cross-sectional view of the spectrometer is shown in Fig. 1. The neutrons enter through the stainless steel window, which was made as thin as possible to reduce neutron scattering, whilst retaining sufficient strength to withstand a maximum pressure differential of 350 kPa (3.5 atm). Designing the window to have a slight curvature provided additional strength, and a thickness of 0.25 mm was possible. To further reduce neutron scattering the amount of the material within the spectrometer was minimised. For example the outer walls and the base of the spectrometer were only 1 mm thick.

The spectrometer was evacuated before filling with the gas mixture of ^{3}He and CO_2. (The 2% partial pressure of CO_2 was added to act as a quench gas.) Choosing materials with good vacuum properties (ie. stainless steel and glass ceramic) and using glass-to-metal or metal-to-metal seals only, it was possible to evacuate the spectrometer to $(8.9 \pm 0.1) \times 10^{-9}$ mbar. Holes were included near the corners of the cathode box to facilitate evacuation of the counter region, and

0   1   2   3   4
Scale cm
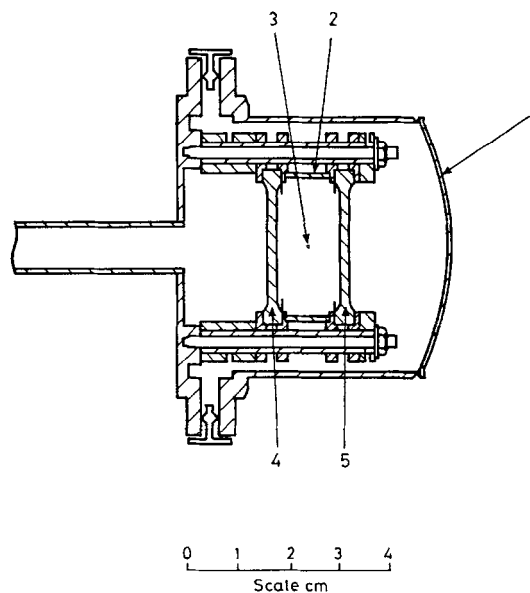
1 Stainless steel window
2 Cathode box
3 Anode wire
4 Back surface barrier detector
5 Front surface barrier detector

Fig. 1. Schematic view of the ^{3}He sandwich spectrometer.

all surfaces that are exposed to the gas, other than the surface barrier detectors, were cleaned ultrasonically to reduce outgassing. This helped to ensure the fill gas was free from impurities, particularly gases with a high electron attachment coefficient (e.g. oxygen and water vapour) which impair the performance of the proportional counter. A tungsten wire of 40 μm diameter was used for the anode which was operated at +650 V.

Both surface barrier detectors had a nominal sensitive area of 450 mm^2, but circular apertures, included to prevent charged particles from striking the edges of the sensitive areas, reduced the effective area to 380 mm^2. The front surface barrier detector, nearest to the stainless steel window, had a depletion depth of 300 μm. However, that of the back surface barrier detector was 500 μm, the greater thickness being necessary to absorb the additional energy of tritons emitted in the same direction as the incident neutrons. The depletion depths were sufficient for total absorption of proton and triton energies for triple coincidence events induced by neutrons of up to 15 MeV.

To perform the energy calibration of the surface barrier detectors, and to enable the gain of the proportional counter signal to be adjusted to give the correct compensation for the energy loss in the gas, an ^{241}Am α-particle source was incorporated in the counter. This source was mounted behind a 2 mm hole in the cathode wall. The mounting unit holding the α-particle source incorporated a 3 mm disc which could be made to roll in front of the hole when the α-particle source was not being used. Further details of the spectrometer design and construction may be found in [1].

2.2. The electronic system

The modular electronic system is shown in Fig. 2. Events were only accepted which produced three signals in coincidence; one from each of the two surface barrier detectors, and one from the proportional counter. In addition, the amplitude of each signal had to be greater than the lower discrimination level set in the single channel analyzers.

An output signal from the fast coincidence unit was only produced if the surface barrier detector signals arrived within the resolving time of 300 ns. A triple coincidence event was then recorded if the delayed output from the coincidence unit was in coincidence with the proportional counter signal. For such events the three signals were digitised and stored on the hard disc of an DEC LSI 11 data acquisition computer, prior to analysis.

3. The efficiency of the ^{3}He spectrometer

The energy dependence of the detector efficiency is required in order to derive the neutron energy spectrum from the measured pulse height spectrum. This dependence was measured in part by the use of a ^{252}Cf source. For this source the neutron energy spectrum in the energy range from 100 keV to 10 MeV is well known and can be described by a Maxwellian distribution with a spectrum parameter $T=1.42$ MeV [18]. The energy dependence of the detector efficiency can, therefore, be determined by comparing the measured pulse height distribution with the known Maxwellian
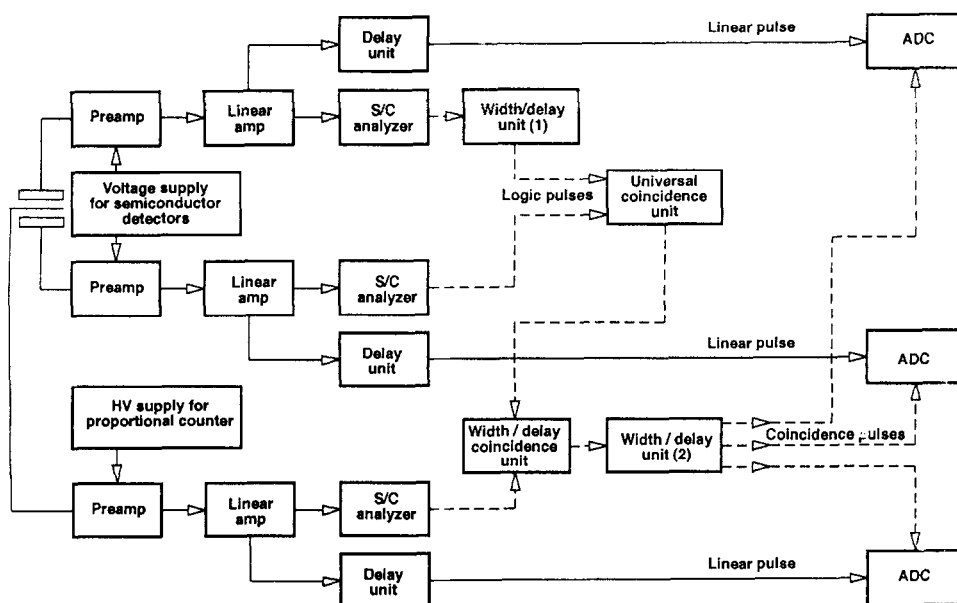

Fig. 2. The modular electronic data acquisition system.

distribution. The result is shown in Fig. 3. The initial increase in the efficiency is associated with the fact that as the neutron energy increases the proton and the triton are less likely to be stopped in the gas and the residual energies are more likely to be greater than the discrimination levels associated with the surface barrier detectors. The decrease is associated with the decrease in the ^{3}He(n,p) cross-section with increasing energy. The uncertainties shown, which are at the 1σ level (68% confidence level), are associated with the counting statistics alone and will produce an uncertainty in the shape of the derived efficiency curve. To minimise these uncertainties an exponential function was fitted to the measured points using the standard least squares method. Above 6.5 MeV the uncertainties due to counting statistics increase rapidly due to the decreasing amplitude in the neutron energy spectrum of the ^{252}Cf source. It was therefore desirable to determine theoretically the form of the efficiency curve in the upper energy region so that measurements could be extended to higher energies.

The Monte Carlo technique was used to calculate the energy dependence of the detector efficiency and
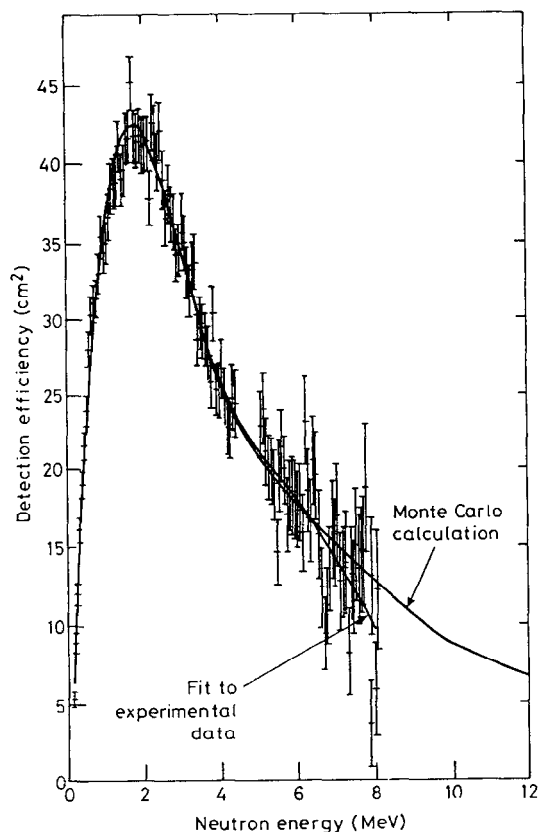
to perform the required extrapolation to higher energies as shown in Fig. 3. In principle the calculation is similar to the work of Bluhm [17] who determined the shape of the efficiency curve for neutron energies up to 5 MeV. However, the present calculations cover a wider energy range: 0.08–20 MeV [1]. The Monte Carlo calculation was also used to determine the optimum gas filling in terms of efficiency for the given energy range, discrimination levels, and the fixed distance between the surface barrier detectors. The operational characteristics of the detector were: gas pressure 200 kPa (about 2 atm), distance between detectors 8 mm. discrimination levels; front detector 0.37 MeV, back detector 0.24 MeV, proportional counter 36 keV.

A by-product of the work on the Monte Carlo calculation was an evaluation of the ^{3}He(n,p)t differential cross-sections from the well known reverse reaction, ^{3}H(p,n)^{3}He. The data, in the energy range 0.08–20 MeV, will be published.

4. Measurement of high resolution neutron energy spectra

Neutron energy spectra were measured for three radioactive (α,n) neutron sources, details of which are given in Table 1. The sources, which are cylindrical, were positioned such that the axis of the cylinder was perpendicular to the axis of the spectrometer. This is the preferred orientation when using these sources because the variation of the emission rate with angle is a minimum in this direction. The distance from the centre of the source to the centre of the active volume of the spectrometer was 6.2 ± 0.1 cm for the Am–Be sources and 4.9 ± 0.1 cm for the Am–B source. At these distances room scattered neutrons were completely negligible.

All measurements were performed in the low scatter facility of the National Physical Laboratory. After each measurement the pulse height spectrum of the ^{252}Cf spontaneous fission source was collected so that the efficiency of the spectrometer could be determined, as described in Section 3.

The pulse height spectrum from the 370 GBq Am–Be neutron source and the background spectrum were each accumulated for 20.25 hr. The resulting neutron energy spectrum is shown in Fig. 4.

The measurement time for the 37 GBq Am–Be source was 45.5 hr and the corresponding background measurement was 42.5 hr. The energy spectrum from this source is shown in Fig. 5. To illustrate the discrimination against gammas and (n,α) reactions in the silicon, the two-parameter spectrum of the acquired data from the 37 GBq Am–Be source is shown in Fig. 6a. The low energy events below the "lower

Fig. 3. Efficiency curve for the ^{3}He spectrometer showing the fit to experimental data and the Monte Carlo calculated extension to higher energies.

Table 1
Details of the neutron sources used in the measurements

| Source	Description	Neutron emission rate $[s^{-1}]$
Americium–beryllium	370 GBq ^{241}Am(α,n) neutron source in an Amersham International Plc X14 capsule (code AMN25). (Stainless steel cylinder, 30.0 mm diameter by 60.0 mm long)	2.126×10^{7}
Americium–beryllium	37 GBq ^{241}Am(α,n) neutron source in an Amersham International Plc X3 capsule (code AMN22). (Stainless steel cylinder, 22.4 mm diameter by 31.0 mm long)	2.424×10^{6}
Americium–boron (natural boron)	37 GBq ^{241}Am(α,n) neutron source in an Amersham International Plc X3 capsule (code AMN22). (Stainless steel cylinder, 22.4 mm diameter by 31.0 mm long)	4.516×10^{5}
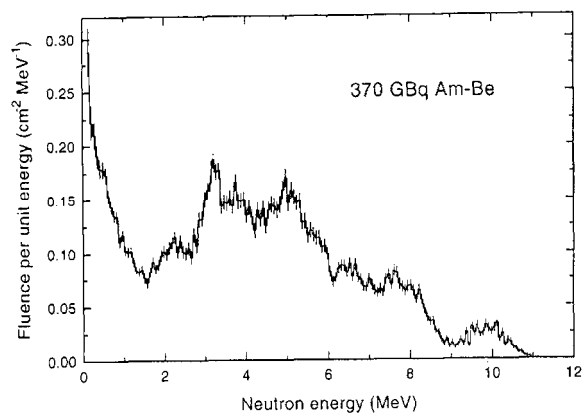
Fig. 4. Measured neutron energy spectrum from the 370 GBq Am–Be neutron source normalized to unit fluence, (uncertainties are due to counting statistics only).
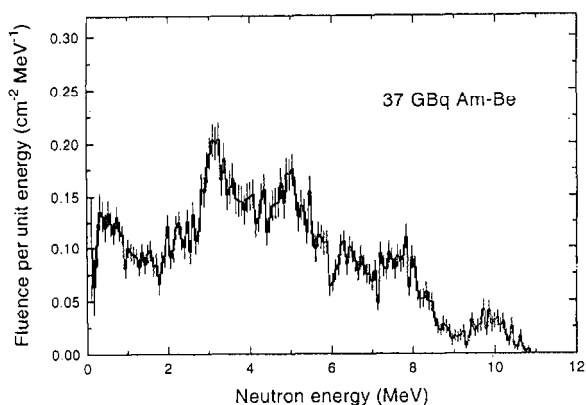

Fig. 5. Measured neutron energy spectrum from the 37 GBq Am–Be neutron source normalized to unit fluence, (uncertainties are due to counting statistics only).
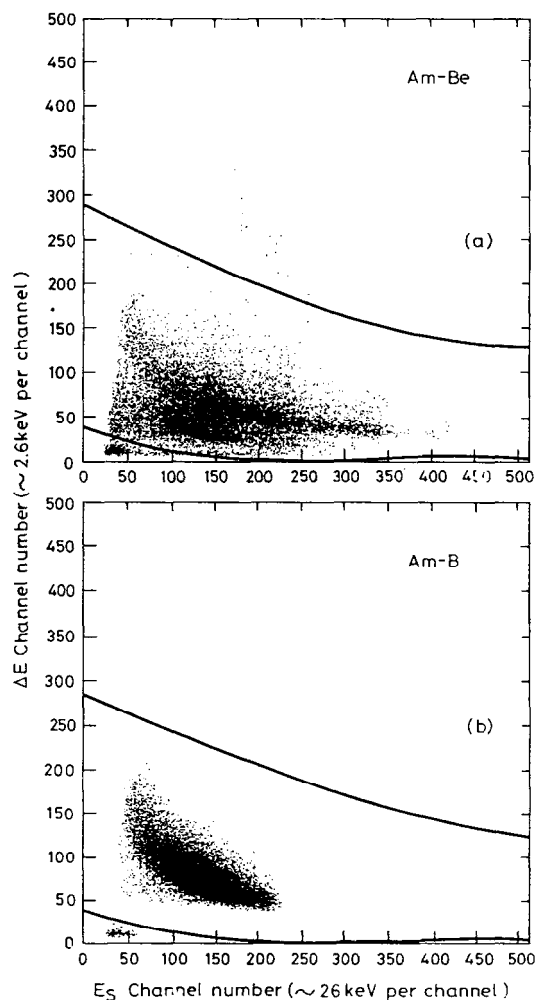

Fig. 6. Two-parameter representation of the total energy E_s versus the energy in the proportional counter ΔE, (a) using the 37 GBq Am–Be source, and (b) using the 37 GBq Am–B source.
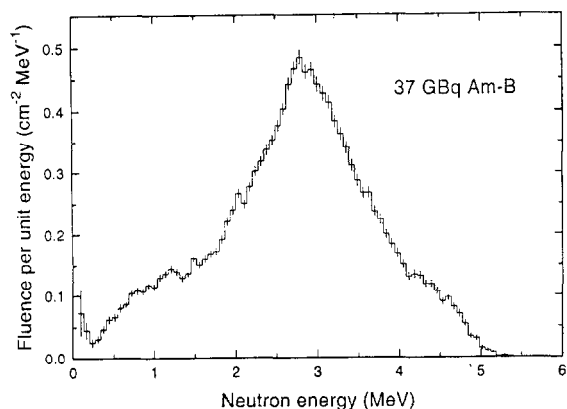
Fig. 7. Measured neutron energy spectrum from the 37 GBq Am–B neutron source normalized to unit fluence, (uncertainties are due to counting statistics only).

table-cut line" in Fig. 6a are associated with photon induced events and electronic noise in the proportional counter. Points above the "upper table cut-line" are from signals originating from the Si(n,α) reaction, ($Q = -2.65$ MeV, [19]). The points between the table cut-lines are due to signals produced by the reactions ^{3}He(n,p) and Si(n,p). The background measurement (i.e. repeat measurement with spectrometer filled with ^{4}He) showed that 34% of these are produced by Si(n,p) reactions. The Q-value for this endothermic reaction [19] is -3.85 MeV and the ^{28}Si(n,p) cross-section [20] peaks between 7.0 MeV and 7.5 MeV.

The neutron energy spectrum from the Am–B source is shown in Fig. 7. With the source strength being relatively low, the measurement time was 12.5 days and for the background measurement, 5 days. The two-parameter spectrum for the Am–B source is shown in Fig. 6b. The separation between the photon events and the ^{3}He(n,p) events is excellent. Because the source strength is relatively low, being an order of magnitude lower than the 37 GBq Am–Be source, the accidental coincidences associated with the neutron reactions in the silicon are negligible. The background measurement showed that less than 0.06% of the signals between the two table cut-lines originate from the Si(n,p) reaction. This is because there are few neutrons above the Si(n,p) reaction threshold.

5. Discussion of the neutron energy spectra

Each of the neutron energy spectra is discussed in turn, and the average neutron energy and various dose equivalent quantities are presented for each one.

5.1. The neutron energy spectrum from a 370 GBq Am–Be source

The measured spectrum in Fig. 4 shows peaks near 2.25, 3.2 5.0, 6.5, 7.7 and 9.9 MeV. All these features can be explained from knowledge of the (α,n) total cross-section [21] and angular distributions [21,22] for beryllium. The neutron production cross-sections for the three individual neutron groups n_0, n_1 and n_2 leaving the ^{12}C nucleus in the ground state, the 4.4 MeV state and the 7.66 MeV state, respectively, are shown in Fig. 8. These cross-sections have been derived from measured angular distributions and 0° differential cross-sections [23]. Preferred neutron energies can be calculated corresponding to resonance alpha energies and preferred angles in the centre of mass system where the angular distributions are strongly anisotropic. These calculated neutron energies are compared with the observed peak energies in Table 2.

As stated in the Introduction, all the peaks above 3 MeV are well established. The peak near 2.25 MeV has not always been recorded by previous measurements. However, Refs. [5,9,16,23] have all indicated a peak near 2.25 MeV and Kluge and Weise [12] have recorded a shoulder at 2.2 MeV. The 2.25 MeV peak may be the result of an increase of intensity at about 40° for the n_2 group angular distribution at $E_\alpha = 5.26$ MeV. Other features associated with the n_2 group are "washed out" by low energy neutrons from the break-up reaction [22,24], from ^{9}Be(α,α')^{9}Be* $\rightarrow$ ^{8}Be+n, and from secondary interactions such as neutron elastic scattering with beryllium and oxygen and the ^{9}Be(n,2n) reactions. Chen Jinxiang [25] et al. have indicated the possibility of a peak at 2.2 McV in the partial neutron spectrum of an Am–Be source measured by time of flight accompanied with the 4.43 MeV gamma ray (i.e. the n_1 group).

The neutron peak at 4.3 MeV identified by Lorch [8] is not seen in the present spectrum (Fig. 4). The origin
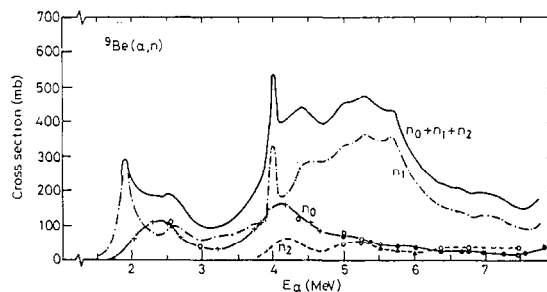

Fig. 8. Neutron production cross sections for the individual neutron groups from the ^{9}Be(α,n)^{12}C reaction (Ref. [21]).

Table 2
Calculated neutron energies for the ^{9}Be$(\alpha,n)^{12}$C reaction

Final ^{12}C state	Alpha energy [MeV]	Preferred c.m. angle	Calculated neutron energy [MeV]	Observed neutron energy [MeV]
Ground state	4.2	0°	9.8	9.9
	4.2	90°	8.0	7.7
	4.2	180°	6.2	6.5
	2.1	0°	7.8	7.7
1st Excited state, 4.43 MeV	4.0	0°	5.0	5.0
	5.1	180°	3.1	3.2
	1.9	0°	3.1	3.2
2nd Excited state, 7.66 MeV	5.3	40°	2.35	2.25

of this peak is not obvious from the (α,n) cross-sections for Be and the associated angular distributions.

5.2. The neutron energy spectrum from a 37 GBq Am–Be source

The spectrum (Fig. 5) shows all the well established peaks above 3 MeV. The peak positions are near 3.2, 5.0. 6.4, 7.7 and 9.9 MeV. Whether a peak exists near 2.2 MeV is difficult to establish due to the large uncertainties from the counting statistics. However, the spectrum does indicate a shoulder in this region.

It can be seen from Fig. 5 that a peak exists in the 0.2 MeV to 1 MeV region. This is compatible with the low energy neutrons from the break-up reaction [22,24] which peaks between 0.2 and 0.3 MeV. Also this peak is in agreement with the measurement made by Werle [15].

Comparing the neutron energy spectra of the two Am–Be neutron sources shown in Fig. 4 and Fig. 5 gives an indication of the dependence of the neutron energy spectrum on source size. Below 0.9 MeV the intensity of the neutrons is greater for the larger source. At higher neutron energies the two spectra agree within counting statistics, with the exception of the peak near 3.2 MeV. This peak for the larger source has a smaller intensity.

The increase in intensity for low energy neutrons for the larger source is expected and is assumed to be due to secondary interactions. Unfortunately, neutron energy spectra calculations [26,27] including the effects of secondary interactions within the source itself, cannot account for the steep low energy rise shown in Fig. 3. However, other published neutron energy spectra measurements of Be(α,n) sources that exceed outer dimensions of 30 mm diameter by 40 mm long show a similar steep rise for low energy neutrons, see, for example, Refs. [5,28,29].

5.3. The neutron energy spectrum from a 37 GBq Am–B source

The measured spectrum (Fig. 7) shows a broad main

peak centred near 2.8 MeV. This peak energy is in agreement with Burger et al. [16] and Werle [15]. A peak/shoulder is indicated near 1.2 MeV. Other workers have failed to find this, probably due to the use of neutron spectrometers of poorer resolution. The prominent shoulder between 4.1 and 4.3 MeV is in agreement with the measurements made by Lorch [8].

The 0° differential cross-sections and the angular distributions for the B$(\alpha,n)^{14}$N reaction have been measured by Van der Zwan and Geiger [30]. From their results they derived the neutron production cross-sections for the three individual neutron groups n_0, n_1 and n_2 resulting from the ^{14}N nucleus being left in the ground state, the 2.31 MeV state and the 3.95 MeV state, respectively. The cross-sections are shown in Fig. 9.

With reference to Fig. 9 there are a number of resonance energies below 5.5 MeV associated with the n_0 group. The angular distributions associated with each of these energies are strongly anisotropic. The overall effect is a preferred neutron emission in the energy range from 2.7 to 3.2 MeV. This accounts for the broad neutron peak centred near 2.8 MeV for the Am–(natural)B spectrum.

The shoulder/peak near 1.2 MeV is caused by the n_1 group, whereas the prominent shoulder between 4.1 and 4.3 MeV is most probably associated with the n_0 group for alpha energies around 5 MeV.
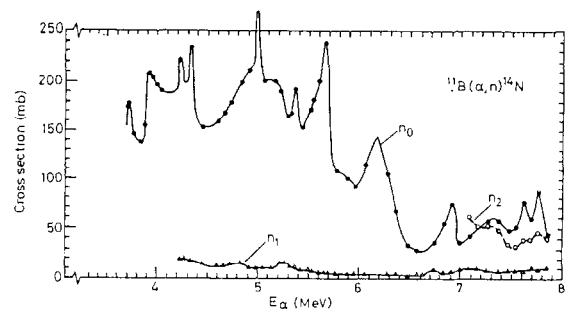

Fig. 9. Neutron production cross sections for the individual neutron groups from the ^{11}B$(\alpha,n)^{14}$N reaction (Ref. [30]).

Table 3
Calculated neutron energies for the $^{11}B(\alpha,n)^{14}N$ reaction

Final ^{14}N state	Alpha resonance energy [30] [MeV]	Preferred c.m. angle	Calculated neutron energy [MeV]
Ground state	3.712	~65°	3.1
	3.94	~105°	2.7
	4.23	~100°	2.9
		~180°	2.2
	4.32	~120°	2.7
	4.98	~15°	4.6
		~115°	3.2
	5.36	~35°	4.9
		~125°	3.2
1st Excited state, 2.313 MeV	3.91	0°	1.2
	4.09	0°	1.3
	4.24	0°	1.5
	4.83	180°	0.7
	5.22	~115°	1.3
	5.28	~130°	1.2

In their cross-section measurements Van der Zwan and Geiger [30] found no evidence of the n_2 group for alpha energies below 5.5 MeV. Therefore the origin of the neutron peak at 340 keV found by Werle [15] is still uncertain. This peak is not seen in the present data, although a rise in neutron intensity is indicated below 200 keV.

The resonance energies and preferred angles for the Am–B reaction are tabulated in Table 3.

5.4. Estimation of average neutron energy and dose equivalent quantities

The average neutron energy and several dose equivalent quantities were calculated for each source. The average dose equivalent conversion factors were calculated from:

$$\bar{H}(10) = \sum_{i=1}^{n} \phi_n(E_i)h(E_i) \quad [\text{Sv cm}^2],$$

where E_i is the neutron energy for energy bin i. $\phi_n(E_i)$ is the normalised fluence for bin i such that

$$\sum_{i=1}^{n} \phi_n(E_i) = 1$$

and $h(E_i)$ is the fluence to dose equivalent conversion factor for energy E_i.

Three sets of fluence-to-dose equivalent conversion factors were used, corresponding to three somewhat different dose equivalent quantities namely:

- MADE (MAximum Dose Equivalent in the ICRU sphere) calculated using conversion factors from ICRP 21 [31],
- ambient dose equivalent [32], calculated using the conversion factors of Wagner et al. [33], which are based on the $Q(L)$ relationship of ICRP 21,
- ambient dose equivalent, calculated using the conversion factors of Leuthold et al. [34], which are based on the revised $Q(L)$ relationship recommended in ICRP 60 [35].

The results are given in Table 4. The uncertainties introduced by the counting statistics of the measured pulse height spectrum are less than 3% in all cases.

Each of the three neutron sources gives a rather similar dose equivalent per unit fluence, because for each source more than 85% of the neutrons emitted are above 1 MeV where the dose equivalent conversion factors do not change much with energy. The dose per unit fluence from the 37 GBq Am–Be neutron source is marginally greater than that of the

Table 4
Average neutron energies and dose equivalent values for the measured neutron spectra

Neutron source	^{241}Am–Be 370 GBq (10 Ci)	^{241}Am–Be 37 GBq (1 Ci)	^{241}Am–B 37 GBq (1 Ci)
Mean energy [MeV]	4.07	4.30	2.70
Dose equivalent (MADE) [31] [pSv cm^2]	372	384	390
Ambient dose equivalent Wagner et al. [33] [pSV cm^2]	380	391	384
Ambient dose equivalent Leuthold et al. [34] [pSv cm^2]	449	457	464

370 GBq Am–Be neutron source because the larger source has a greater relative number of neutrons below 1 MeV.

The value of 372 pSv cm^2 for MADE for the 37 GBq source compares well with the value of 375 pSv cm^2 obtained by Kluge and Weise [12] for this quantity for a source of similar total emission rate. The change from MADE to ambient dose equivalent as based on the conversion factors of Wagner et al. results in very little change for these sources. On going to the new ambient dose equivalent values based on the conversion factors of Leuthold et al. the increase is 17–18% for Am–Be and 21% for Am–B.

6. Conclusion

High resolution measurements of neutron energy spectra from Am–Be and Am–B neutron sources have been carried out with a ^{3}He sandwich spectrometer. A qualitative explanation of the observed peaks/shoulders has been discussed by considering the total cross-sections and angular distributions for the neutron production reactions. The spectra have also been compared with previous measurements of other workers, and the main features of each spectrum are in good agreement. The spectra, either in tabular form, or on a computer diskette can be obtained from the authors.

Acknowledgments

References

[1] J.W. Marsh, Ph.D Thesis, Council for National Academic Awards (1990).

[2] R. Birch, Thesis, University of Birmingham (1988).

[3] M.N. Thompson and J.M. Taylor, Nucl. Instr. and Meth. 37 (1965) 305.

[4] P. Cloth and R. Hecker, Nukleonik 12 (1969) 163.

[5] H. Kluge, K. Weise and H.W. Zill, Neutron Monitoring for Radiation Protection Purposes, IAEA-SM-167/7, Vienna, December 1972.

[6] E. Lehman, Nucl. Instr. and Meth. 60 (1968) 253.

[7] F.X. Haas and J.T. McCarthy, Nucl. Instr. and Meth. 50 (1967) 340.

[8] E.A. Lorch, Int. J. Appl. Radiation and Isotopes 24 (1973) 585.

[9] H. Kluge, Z. Naturforsch. 24a (1969) 1289.

[10] S. Notarrigo, F. Porto, A. Rubbino and S. Sambataro, Nucl. Phys. A 125 (1969) 28.

[11] L. Van der Zwan, Can. J. Phys. 46 (1968) 1527.

[12] H. Kluge and K. Weise, Radiat. Prot. Dosim. 2 (1982) 85.

[13] K.W. Geiger and C.J.D. Jarvis, Can. J. Phys. 40 (1961) 33.

[14] H. Bluhm and D. Stegemann, Nucl. Instr. and Meth. 70 (1969) 141.

[15] H. Werle, Karlsruhe INR-4/70/25 (1970).

[16] G. Burger, W. Eckl and H. Gredel, Advances in Physical and Biological Radiation Detectors, IAEA-SM-143/15, Vienna (1971) p. 467.

[17] H. Bluhm, Nucl. Instr. and Meth. 115 (1974) 325.

[18] International Organisation for Standardisation, ISO 8529, 1989.

[19] R.G. Miller and R.W. Kavanagh, Nucl. Instr. and Meth. 48 (1967) 13.

[20] D.I. Garber and R.R. Kinsey, Neutron Cross Sections, Brookhaven National Laboratory, BNL 325 (1976) p. 2.

[21] L. Van der Zwan and K.W. Geiger, Nucl. Phys. A 152 (1970) 481.

[22] A.W. Obst, T.B. Grandy and J.L. Weil, Phys. Rev. C 5 (1972) 738.

[23] K.W. Geiger and L. Van der Zwan, Int. J. Appl. Radiation and Isotopes 21 (1970) 193.

[24] H. Werle, L. Van der Zwan and K.W. Geiger, Z. Physik 259 (1975) 275.

[25] C. Jinxiang, T. Guoyou, B. Shanglian, Z. Wenguang and S. Zhaomin, International Atomic Energy Agency, INDC(CPR)-004/L (1985).

[26] A.D. Vijaya and A. Kumar, Nucl. Instr. and Meth. 111 (1973) 435.

[27] A. Kumar and P.S. Nagarajan, Nucl. Instr. and Meth. 140 (1977) 175.

[28] M.E. Anderson and W.H. Bond, Nucl. Phys. 43 (1963) 330.

[29] M.E. Anderson and R.A. Neff, Nucl. Instr. and Meth. 99 (1972) 231.

[30] L. Van der Zwan and K.W. Geiger, Nucl. Phys. A 246 (1975) 93.

[31] ICRP, Publication 21, Data for Protection against Ionizing Radiation from External Sources, International Commission on Radiological Protection (Pergamon, Oxford, 1973).

[32] ICRU, Report 39, Determination of Dose Equivalents Resulting from External Radiation Sources, International Commission on Radiation Units and Measurements (ICRU Publications 1985).

[33] S.R. Wagner, B. Grosswendt, J.R. Harvey, A.J. Mill, H.-J. Selbach and B.R.L. Siebert, Radiat. Prot. Dosim. 12 (1985) 231.

[34] G. Leuthold, V. Mares and H. Schraube, Radiat. Prot. Dosim. 40 (1992) 77.

[35] ICRP, Publication 60, 1990 Recommendations of the International Commission on Radiological Protection, Annals of the ICRP 21 (1991) No. 1–3, International Commission on Radiological Protection (Pergamon, Oxford).